International Journal of Control, Automation, and Systems VV(X) (YYYY) 1-3
http://dx.doi.org/10.1007/s12555-xxx-xxxx-xx
ISSN:1598-6446 eISSN:2005-4092
http://www.springer.com/12555

Sparse Identification and Nonlinear Model Predictive Control for Diesel Engine Air Path System

Shuichi Yahagi*, Hiroki Seto, Ansei Yonezawa, and Itsuro Kajiwara

Abstract: This paper presents a sparse identification of nonlinear dynamic systems (SINDy) for a diesel engine air path system and nonlinear model predictive control (NMPC) with the SINDy model to attain good control performance. The air path system control is well known as a challenging problem, and many studies have been presented such as traditional model-based control design and machine learning. However, these conventional approaches still have some difficulties including the control performance and design costs. In this paper, we obtain the model of the air path system in a data-driven manner using the SINDy algorithm and construct the offset-free NMPC with the SINDy model. SINDy is a suitable modeling method for controlling a complicated air path system, owing to its characteristics of high computational efficiency, high learning efficiency, high modeling accuracy, and applicability to complex systems. Additionally, NMPC provides high control performance under constraints. The proposed offset-free NMPC with the SINDy model is verified through the simulations. The results show that the coefficient of determination of the SINDy model provided over 90%, and the controller performance of the NMPC was better than that of the traditional robust controller and satisfied the constraints.

Keywords: Air path system, Diesel engine, Model predictive control, Sparse identification.

1. INTRODUCTION

Studies on model-based control have been actively conducted in the automotive and control fields. In model-based control, the controller is designed based on a mathematical model. Thus, the controller performance depends on the accuracy of the model. Traditional system identification, including the ARX model and Numerical Algorithms for State Space Subspace System Identification (N4SID) [1], is highly effective for linear systems. However, system identification for industrial systems with strong nonlinearity is a challenging problem, making it difficult to control complex industrial systems. To address this problem, data-driven control which actively uses data has been proposed in recent years [2]. Data-driven control can be broadly divided into two types. One is a direct method that designs a controller without modeling the controlled object, and the other is an indirect method that designs a controller using a model obtained from data-driven modeling. As direct methods, virtual reference feedback tuning (VRFT) [3], fictitious reference iterative tuning (FRIT) [4], and correlation-based tuning (CbT) [5] have been proposed. These methods are useful for industrial systems and many applications have also been progressing [6]–[12]. On the other hand, modeling is still essential in terms of preliminary consideration before implementing controllers and the use of knowledge of conventional model-based control designs. Therefore, there is a high demand for design methods that use plant models (i.e., indirect methods).

Various data-driven modeling studies have been conducted for controlled targets whose physical modeling is difficult [2], [13]. Conventional machine learning approaches, including deep learning and reinforcement learning, have been proposed to achieve the desired control over such complex systems. Nevertheless, computational and learning costs are problematic. To solve this problem, various methods have been examined in the field of data-driven science, such as dynamic mode decomposition (DMD) [14], [15], Koopman analysis [13], [16]–[18], and sparse identification of nonlinear dynamical systems (SINDy) [19]. Especially, SINDy

Manuscript received January 10, 2021; revised March 10, 2021; accepted May 10, 2021. Recommended by Associate Editor Soon-Shin Lee under the direction of Editor Milton John. This journal was supported by the Korean Federation of Science and Technology Societies Grant.

Shuichi Yahagi and Hiroki Seto are with 6th Research Department, ISUZU Advanced Engineering Center Ltd., 8 Tsutidana, Fujisawa-shi, Kanagawa 252-0881, Japan (e-mails: {shuichi_yahagi, hiroki_seto}@isuzu.com). Ansei Yonezawa was with Division of Mechanical and Aerospace Engineering, Hokkaido University, N13, W8, Kita-ku, Sapporo, Hokkaido 060-8628, Japan. He is now with Department of Mechanical Engineering Faculty of Engineering, Kyushu University, 744 Motooka, Nishi-ku, Fukuoka 819-0395, Japan (e-mails: ayonezawa@mech.kyushu-u.ac.jp). Itsuro Kajiwara is with Division of Mechanical and Aerospace Engineering, Hokkaido University, N13, W8, Kita-ku, Sapporo, Hokkaido 060-8628, Japan (e-mails: ikajiwara@eng.hokudai.ac.jp).
* Corresponding author.

features sparse modeling which suppresses overfitting and reduces computational costs [20]. Furthermore, it has been shown to have a lower computational load than neural networks and higher modeling accuracy than DMD. Owing to these characteristics, SINDy is known to be compatible with model predictive control [21], which achieves desired control with satisfying constraints by performing optimization in real-time [22]–[26].

Previous literature about applications of SINDy has shown that SINDy is highly effective for nonlinear multi-input multi-output (MIMO) systems like Lorenz equations and susceptible-exposed-infectious-removed epidemic models. Furthermore, applications to industrial systems have also been considered. To date, SINDy has developed chemical process models, including a continuous stirred tank reactor [27], distillation column [28], hydraulic fracturing [29], and isothermal batch reactor [30]. In addition to chemical processes, SINDy-based algorithms have also been applied to fluid dynamics [19], physics [31], and biology [32] to obtain the governing equations and dynamical systems [19], [21], [33], [34]. However, there are few examples of its application to industrial products including automotive systems. In this paper, we examine the applicability of the SINDy algorithm to the intake and exhaust system of a diesel engine, which is known to be a complex MIMO system with strong nonlinearity. Since achieving the desired control is a challenging issue for such a system, various controller design methods have been proposed [35]–[39]. In this study, we model the intake and exhaust system of a diesel engine using SINDy and use the obtained nonlinear differential equation to apply nonlinear model predictive control (NMPC). The application of SINDy to intake and exhaust systems of diesel engines has not been studied, to the best of our knowledge. The contributions of this paper are summarized as follows:

- SINDy is applied to the intake and exhaust system of a diesel engine, known as a complex MIMO system. To the best of the authors' knowledge, the proposed approach has not previously been conducted on the diesel engine, and this study provides new insights for researchers and practical engineers.
- NMPC with the prediction model obtained by SINDy is constructed. Additionally, an offset-free NMPC is realized by introducing an augmented system with a variable of integral error between target and response to reduce the steady-state error.

We describe the structure of this paper. Section 2 explains the intake and exhaust system of the internal combustion engine, which is the controlled object. In data-driven modeling, a model is created from data, so we will omit detailed explanations of physical formulas and limit ourselves to an overview of the system. Section 3 describes SINDy, which is one of the data-driven modeling methods, for the diesel engine air path system. In Section 4, we will build an offset-free NMPC that can reduce steady-state error. In Section 5, we compare the proposed method with the conventional one through simulation. Section 6 provides a summary of this paper.

2. AIR PATH SYSTEM OF DIESEL ENGINE

The control target is the intake and exhaust system of the 4-cylinder diesel engine shown in Fig. 1. This system has an exhaust gas recirculation (EGR) system and a variable geometry turbocharger (VGT). EGR has the role of appropriately adjusting the oxygen concentration taken into the cylinder. By mixing exhaust gas containing lean oxygen with fresh air, the oxygen concentration is kept low. This reduces the peak temperature during combustion and suppresses the amount of harmful nitrogen oxides that are often produced at high temperatures. VGT has the role of appropriately adjusting the pressure inside the intake manifold. When the movable vane spacing is narrowed, the flow path is narrowed and the flow velocity increases, resulting in a supercharging effect can be obtained from low rotation speeds. In the high rotation range, the vane spacing is widened to allow the exhaust to flow more easily. Next, we explain the flow of gas. Fresh air drawn in from outside is compressed by a compressor, cooled by an intercooler, then passes through the intake throttle and flows into the intake manifold. Gas that passes through the EGR valve also flows into the intake manifold. The oxygen concentration in the gas inside the intake manifold is controlled by operating the EGR valve. Gas in the intake manifold flows into the cylinder, and after combustion, the gas is discharged to the exhaust manifold. The gas that leaves the exhaust manifold is divided into two paths: one is recirculated through the EGR cooler, and the other is the exhaust gas through the turbine. The gas after combustion passes through the exhaust manifold and operates the turbine. Then, the state of the turbine rotation speed is controlled by manipulating the turbine vane angle. This EGR system is called high-pressure EGR, and it is a mechanism that returns relatively high-temperature gas from upstream of the turbine to the intake manifold.

For this system, we aim to control boost pressure and EGR rate by manipulating the VGT vane and EGR valve under the various operating points (fuel injection amounts and engine speeds). However, there are issues such as nonlinearity and actuator constraints, strong interference in the air path between the EGR and VGT, and characteristics that vary depending on operating conditions. Thus, many studies of the air path system control have been conducted [35], [36], [39], [40]. In this study, we adopt data-driven modeling, so explanations regarding physical modeling will be omitted. For details, refer to reference [41].

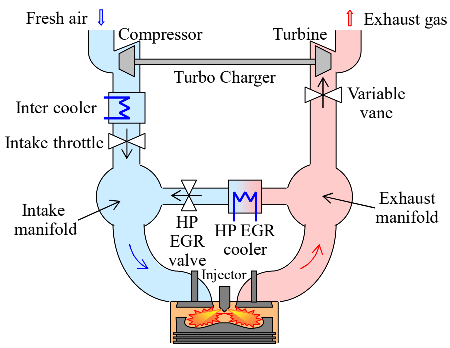

Fig. 1. Air path system of diesel engine.

3. SPARSE IDENTIFICATION

3.1. SINDy with control input

SINDy with control input has been proposed as a data-driven modeling method for nonlinear systems. SINDy has desirable features for practice, including high computational efficiency, high learning efficiency, high modeling accuracy, and applicability to complex systems. Herein, we explain SINDy with input based on literature [21], [34]. Consider the following nonlinear dynamic system with the control input:

$$x(k+1) = f_p\big(x(k), u(k)\big) \tag{1}$$

where $f_p: \mathbb{R}^n \times \mathbb{R}^l \to \mathbb{R}^n$ is a smooth nonlinear function, $x(k) = [x_1(k) \quad x_2(k) \quad \cdots \quad x_n(k)\ ]^T \in \mathbb{R}^n$ is the state vector, $u(k) = [u_1(k) \quad u_2(k) \quad \cdots \quad u_l(k)\ ]^T \in \mathbb{R}^l$ is the control input vector, and $t_k = k\Delta t$. Then, the snapshot data $X \in \mathbb{R}^{m\times n}$ and $\Gamma \in \mathbb{R}^{m\times l}$ for the length of data, m, are given as

$$X = \begin{bmatrix} - \ x^T(1) \ - \\ - \ x^T(2) \ - \\ \vdots \\ - \ x^T(m) \ - \end{bmatrix} \in \mathbb{R}^{m\times n}, \tag{2}$$

$$X^+ = \begin{bmatrix} - \ x^T(2) \ - \\ - \ x^T(3) \ - \\ \vdots \\ - \ x^T(m+1) \ - \end{bmatrix} \in \mathbb{R}^{m\times n}, \tag{3}$$

$$\Gamma = \begin{bmatrix} - \ u^T(1) \ - \\ - \ u^T(2) \ - \\ \vdots \\ - \ u^T(m) \ - \end{bmatrix} \in \mathbb{R}^{m\times l}. \tag{4}$$

Introducing the basis function $\Theta_p: \mathbb{R}^{m\times n} \times \mathbb{R}^{m\times l} \to \mathbb{R}^{m\times p}$ which is called library or dictionary, the dynamics can be expressed as

$$X^+ = \Theta_p(X, \Gamma)\Xi, \tag{5}$$

where $\Xi \in \mathbb{R}^{p\times n}$ is a coefficient matrix give as

$$\Xi = \begin{bmatrix} | & | & | & | \\ \xi_1 & \xi_2 & \cdots & \xi_n \\ | & | & | & | \end{bmatrix} \in \mathbb{R}^{p\times n}. \tag{6}$$

The various basis function $\Theta_p(X,\Gamma)$ can be selected by a user. For instance, the basis function $\Theta_p(X,\Gamma)$ is set as

$$\Theta_p(X,\Gamma) = [1 \quad X \quad \Gamma \quad X\otimes X \quad X\otimes\Gamma \quad \cdots \quad \sin(X) \quad \sin(\Gamma) \quad \sin(X\otimes X) \quad \sin(X\otimes\Gamma) \quad \cdots], \tag{7}$$

where $\otimes$ represents the Kronecker product and $X\otimes X$ is second order cross-term, given by

$$X\otimes X = \begin{bmatrix} x_1^2(1) & x_1x_2(1) & \cdots & x_2^2(1) & \cdots & x_n^2(1) \\ x_1^2(2) & x_1x_2(2) & \cdots & x_2^2(2) & \cdots & x_n^2(2) \\ \vdots & \vdots & \vdots & \vdots & \vdots & \vdots \\ x_1^2(m) & x_1x_2(m) & \cdots & x_2^2(m) & \cdots & x_n^2(m) \end{bmatrix}. \tag{8}$$

Furthermore, by adding a regularization term to suppress overfitting and compress data, the following optimization problem is obtained:

$$\xi_i = \arg\min_{\xi_i'} \|X_i^+ - \Theta(X,\Gamma)\xi_i'\|_2^2 + \lambda_0\|\xi_i'\|_0 \tag{9}$$

where ξ_i represents the i-column vector of Ξ, X_i^+ represents the i-column component of X^+ and λ_0 represents the sparsity-promoting hyperparameter that is tuned through an experiment to result in the best estimation of the dynamics. In this optimization problem, a sparsified coefficient vector ξ_i is obtained by LASSO (least absolute shrinkage and selection operator) regression [42] or STLS (sequentially thresholded least-squares) [16]. Using the obtained coefficient matrix Ξ, the dynamic system is described as

$$x(k+1) = \Xi^T\left(\vartheta_p\big(x^T(k), u^T(k)\big)\right)^T, \tag{10}$$

where $\vartheta_p: \mathbb{R}^n \times \mathbb{R}^l \to \mathbb{R}^p$ is the vector function corresponding to the matrix function Θ_p, given as

$$\vartheta_p(x^T, u^T) = [1 \quad x^T \quad u^T \quad x^T\otimes x^T \quad x^T\otimes u^T \quad \cdots \quad \sin(x^T) \quad \sin(u^T) \quad \sin(x^T\otimes x^T) \quad \cdots \quad \sin(x^T\otimes u^T) \quad \cdots\ ]. \tag{11}$$

3.2. SINDy for air path system

Based on the explanation in Section 2, the input-output relationship of the intake and exhaust system is summarized (see Table 1). The states x_1 and x_2 are the intake manifold pressure (boost pressure) [kPa] and EGR rate [%], respectively. The inputs u_1 and u_2 are the VGT vane closure [%, closing] and EGR valve opening [%, opening], respectively. Fuel injection volume [mm^3/st] and engine speed [rpm] are signals determined by the driver's operation and are defined as exogenous inputs d_1 and d_2, respectively. It is noted that the output y is the same as the state vector x, which is measurable. Therefore, a dynamic system with the exogenous input is given as

$$x(k+1) = f\big(x(k), u(k), d(k)\big), \tag{12}$$

$$y(k) = h\big(x(k)\big) = x(k), \tag{13}$$

where $f: \mathbb{R}^n \times \mathbb{R}^l \times \mathbb{R}^q \to \mathbb{R}^n$ and $h: \mathbb{R}^n \to \mathbb{R}^n$ are smooth nonlinear functions, and $d(k) = [d_1(k) \quad d_2(k) \quad \cdots \quad d_q(k)\ ]^T \in \mathbb{R}^q$ is the exogenous input vector. The snapshot data $D \in \mathbb{R}^{m\times q}$ is given as

$$D = \begin{bmatrix} - \ d^T(1) \ - \\ - \ d^T(2) \ - \\ \vdots \\ - \ d^T(m) \ - \end{bmatrix} \in \mathbb{R}^{m\times q}. \tag{14}$$

As in the previous section, if we set the basis function $\Theta: \mathbb{R}^{m\times n} \times \mathbb{R}^{m\times l} \times \mathbb{R}^{m\times q} \to \mathbb{R}^{m\times p}$ with the snapshot data D added to (7), the dynamics can be expressed as

$$X^+ = \Theta(X, \Gamma, D)\Xi. \tag{15}$$

As in (9), the optimization problem is given by

$$\xi_i = \arg\min_{\xi_i'} \| X_i^+ - \Theta(X, \Gamma, D)\xi_i' \|_2^2 + \lambda_0 \|\xi_i'\|_0 . \quad (16)$$

Using the coefficient matrix Ξ which is a decision variable, the dynamic system is described as

$$x(k+1) = \Xi^T \left(\vartheta(x^T(k), u^T(k), d^T(k)) \right)^T , \quad (17)$$

where ϑ: $\mathbb{R}^n \times \mathbb{R}^l \times \mathbb{R}^q \to \mathbb{R}^p$ is a vector function corresponding to the matrix function Θ.

Table 1. Parameters.

Variable	Description	Unit
x_1	Boost pressure	Pa
x_2	EGR rate	%
u_1	VGT vane	%
u_2	EGR valve	%
d_1	Fuel injection amount	mm³/st
d_2	Engine speed	rpm

4. CONTROLLER DESIGN

Herein, we construct the NMPC with SINDy model. In addition, an augmented system in which the integral of the deviation e^{int} is added to (17) to remove the steady-state error is introduced as follows:

$$\begin{cases} x(k+1) = \Xi^T \left(\vartheta(x^T(k), u^T(k), d^T(k)) \right)^T \\ e^{int}(k+1) = e^{int}(k) + \left(r(k) - x(k) \right) \end{cases} . \quad (18)$$

Based on this equation, the optimization problem of the proposed offset-free NMPC is given by

$$\min_{u(0), u(1), \cdots, u(H_u)} J , \quad (19)$$

$$J = \sum_{i=0}^{H_p - 1} \| r(k) - x(k+i) \|_Q^2 + \| e^{int}(k+i) \|_{Q_e}^2 + \| u(k+i) \|_{R_u}^2 + \| \Delta u(k+i) \|_{R_{\Delta u}}^2 \quad (20)$$

subject to

$$\begin{cases} x(i+1) = \Xi^T \left(\vartheta(x^T(i), u^T(i), d^T(k)) \right)^T \\ e^{int}(i+1) = e^{int}(i) + \left(r(k) - x(i) \right), e^{int}(0) = 0 \end{cases}$$
$$u_{min} \le u(i) \le u_{max}, i = 0, \dots, H_p - 1$$
$$u(i) \equiv u(H_u), i = H_u, \dots, H_p - 1. \quad (21)$$

where $\Delta u(i) = u(i) - u(i-1)$; r is target value; Q, Q_e, R_u, and $R_{\Delta u}$ are positive definite diagonal matrices, and are the weights for the deviation, the integral of the deviation, the control input, and the amount of change in the control input, respectively; $\|\bullet\|_Q^2$ represents the weighted 2-norm of Q, defined as $\|x\|_Q^2 = x^T Q x$; H_p and H_u are the prediction horizon and control horizon, respectively. The solver uses Sequential Quadratic Programming (SQP). Note that in MPC, the first control input $u(0)$ obtained by solving the optimization problem is used as the control input.

5. SIMULATION RESULTS

5.1. Data acquisition and modeling

The plant model of the air path system is a mean value model constructed in MATLAB/Simulink. The frequency characteristics under various operating points are shown in Appendix A. Herein, the one-step prediction is defined as

$$\begin{cases} \hat{x}(k+1) = \Xi^T \left(\vartheta(x^T(k), u^T(k), d^T(k)) \right)^T \\ \hat{y}(k) = h(\hat{x}(k)) \end{cases} , \quad (22)$$

where $\hat{y}$ is the predicted value of y. In the one-step prediction, given the data at time step k, the state at time step $k+1$ is predicted. The long-term prediction is defined as

$$\begin{cases} \hat{x}(k+1) = \Xi^T \left(\vartheta(\hat{x}^T(k), u^T(k), d^T(k)) \right)^T \\ \hat{y}(k) = h(\hat{x}(k)) \end{cases} \quad (23)$$

with $\hat{x}(0) = x(0)$. In the long-term prediction, given the inputs at time step k and the initial state, the state over time step $k+1$ is predicted. Even if the accuracy of the one-step prediction is high, that of long-term prediction may not necessarily be good because the optimization problem evaluates only one-step prediction (see Table 2 and Table 3 indicated below). Fig. 2 shows the learning data acquired for modeling the air path system and the predictive data computed from the SINDy model. Fig. 3 shows the detail of Fig. 2. It is noted that the predicted data are the long-term prediction, not the one-step prediction. In the figures, y_1, y_2, e_1, e_2, u_1, u_2, d_1, and d_2 are intake manifold pressure, EGR rate, prediction error of boost pressure, prediction error of EGR rate, VGT valve, EGR valve, fuel injection amount, and engine speed, respectively. The dotted lines represent the predicted values, and the solid lines represent actual values. Signals of VGT vane closure, EGR valve opening, fuel injection amount, and engine speed generated by Design of Experiments (DoE) using the Sobol quasi-random number method are applied to the plant, and the intake manifold pressure and EGR rate are obtained. The sampling period is 0.01 s, and the number of sampling points is 5×10^5. The basis function was set to a second-order polynomial. We use STLS algorithm [16] to solve the optimization problem (16). In STLS, λ, called the sparsification knob, is used as the parameter corresponding to λ_0. Table 2 and Table 3 show the coefficient of determination R^2 of the one-step and the long-term predictions for multiple λ, respectively. The coefficient of determination R^2 of $z \in \mathbb{R}$ is defined as

$$R^2 = 1 - \frac{\sum_{k=1}^N \left(z(k) - \hat{z}(k) \right)^2}{\sum_{k=1}^N (z(k) - \bar{z})^2} , \quad (24)$$

where $\hat{z}$ and $\bar{z}$ are the predicted and the mean values of z, respectively. The metric value, R^2, is close to the unit when the accurate model is obtained. The negative value of this metric means that the model has a low accuracy [43]. In general, when the value is over 90%, R^2 is acceptable in an engineering perspective [44]. Table 4 shows the number of nonzero elements of the coefficient matrix Ξ. From Table 2, the R^2 values of the one-step predictions are more than 0.99 for the intake manifold pressure and EGR rate. From Table 3, R^2 of the long-term predictions depends on λ. Note that the negative value in the table means that the obtained model has low accuracy [43]. When λ is 1×10^{-6}, the predicted response is unstable due to overlearning. When λ is 4×10^{-5}, prediction accuracy is low. This is because the identified model became too sparse to express the nonlinearity of the system. From the results, $\lambda = 2 \times 10^{-5}$ is suitable. It can be confirmed that highly accurate modeling is achieved using SINDy. We also confirmed that the obtained SINDy model provides a good prediction for 2500 s dataset with different learning data. This data was generated by random signals. The R^2 values of long-term prediction for the intake manifold pressure and EGR rate are 0.952 and 0.983, respectively. Fig. 4 shows the identified coefficient matrix when $\lambda = 2 \times 10^{-5}$. The white parts in the figure indicate zero, which means the identified coefficient matrix is sparsified due to SINDy modeling. From the figure, we can see the elements of the library (i.e., basis function) that are of high importance for creating this model. Considering the figure from a controller design perspective, the visualization of the coefficient matrix shows the effect of linear coupling is strong. This is also implied by the fact that a linear-time invariant (LTI) control designed using the linearized model can be applied to the air path system, as described in the next subsection. On the other hand, the visualized coefficient matrix shows the air path system is essentially nonlinear since the many nonlinear elements of the library do not indicate zero. This leads to limitations in the performance of the LTI controller. Therefore, it is essential to introduce the nonlinear controller to achieve high control performance of the diesel engine air path system, and the NMPC has been presented in Section 4.

Table 2. R^2 of one-step prediction.

λ [$\times 10^{-5}$]	y_1	y_2
0.1	0.999	0.999
1	0.999	0.999
2	0.999	0.999
3	0.999	0.999
4	0.999	0.999

Table 3. R^2 of long-term prediction.

λ [$\times 10^{-5}$]	y_1	y_2
0.1	unstable	unstable
1	0.9278	0.9810
2	0.9384	0.9823
3	0.9205	0.9822
4	−12.03	0.8772

Table 4. The number of nonzero elements of Ξ.

λ [$\times 10^{-5}$]	0.1	1	2	3	4
N	56	48	43	41	35

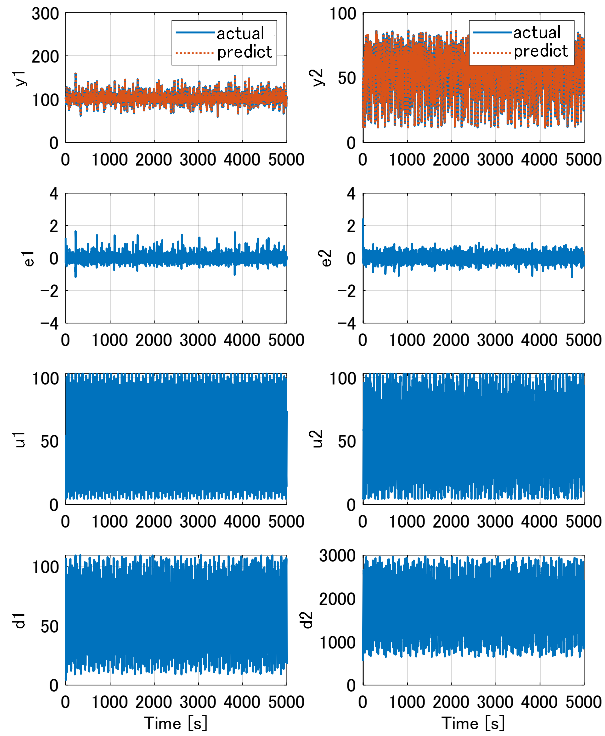

Fig. 2. Learning data and predictive accuracy. y_1: boost pressure [kPa], y_2: EGR rate [%], e_1: prediction error of boost pressure [kPa], e_2: prediction error of EGR rate [%], u_1: VGT vane [%, closing], u_2: EGR valve [%, opening], d_1: fuel injection amount [mm^3/st], d_2: engine speed [rpm].

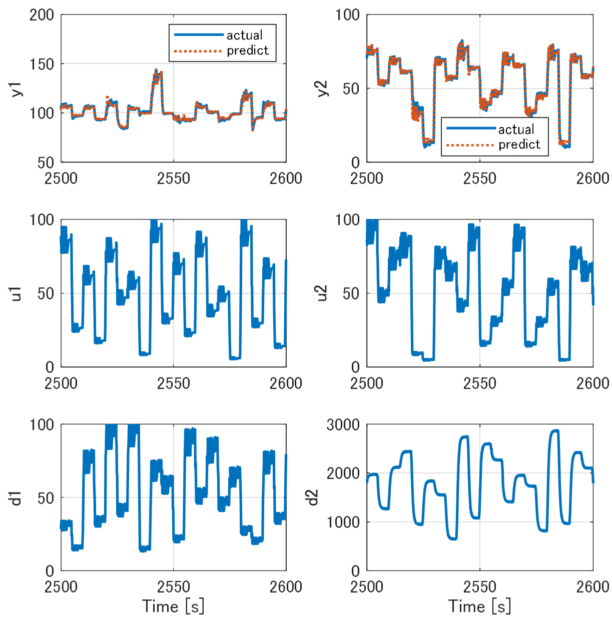

Fig. 3. The detail of learning data and predictive accuracy. y_1: boost pressure [kPa], y_2: EGR rate [%], u_1: VGT vane [%, closing], u_2: EGR valve [%, opening], d_1: fuel injection amount [mm^3/st], d_2: engine speed [rpm].

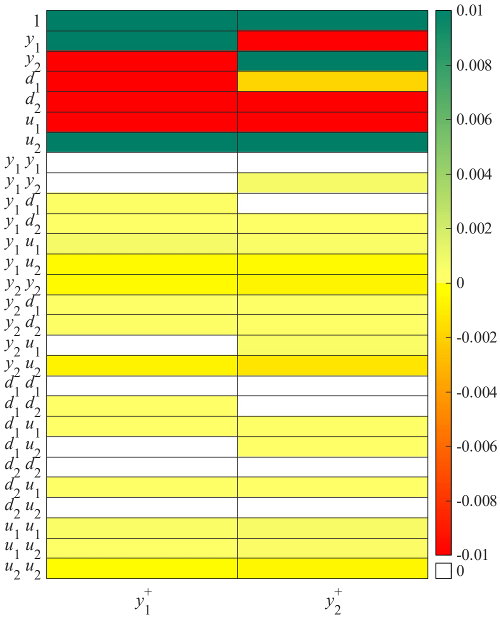

Fig. 4. Visualization of identified coefficient matrix Ξ ($\lambda = 2 \times 10^{-5}$).

5.2. The performance of NMPC

Fig. 5 shows the results of applying NMPC. Table 5 shows the setting of the design parameters. In addition, results of the LTI H_∞ control are also shown to confirm the validity of the NMPC performance. In the figure, the broken lines represent the target value, the solid lines represent the proposed offset-free NMPC, and the dotted lines represent the H_∞ control. The H_∞ controller was designed from a linear model derived at multiple operating points (81 points in total) by setting one operating point as the nominal model and the other operating points as multiplicative uncertainties with respect to the nominal model. The order of the controller is 10. From the figure, we can see that NMPC achieves good control performance with small steady-state errors. Table 6 shows the MSEs of the offset-free NMPC and LTI H_∞ controllers. MSEs for the boost pressure and EGR rate under NMPC are 3.35 and 1.05, respectively. MSEs for those under H_∞ control are 11.5 and 1.24, respectively. Thus, it can be confirmed that the offset-free NMPC provides higher control performance than LTI H_∞ control. Next, in order to confirm whether the actuator constraints were satisfied, a simulation was performed under the different conditions of the exogenous inputs (i.e., fuel injection amount and engine speed). The results are shown in Fig. 6. Checking the VGT vane signal (u_1) around 80 s, it is confirmed that the VGT vane satisfies the actuator constraint without exceeding 100%.

Table 5. Design parameters.

Parameter	Value
H_p	30
H_u	3
Q	diag (20, 20)
Q_e	diag (0.5, 1.0)
R_u	diag (0.001, 0.001)
$R_{\Delta u}$	diag (500, 1000)

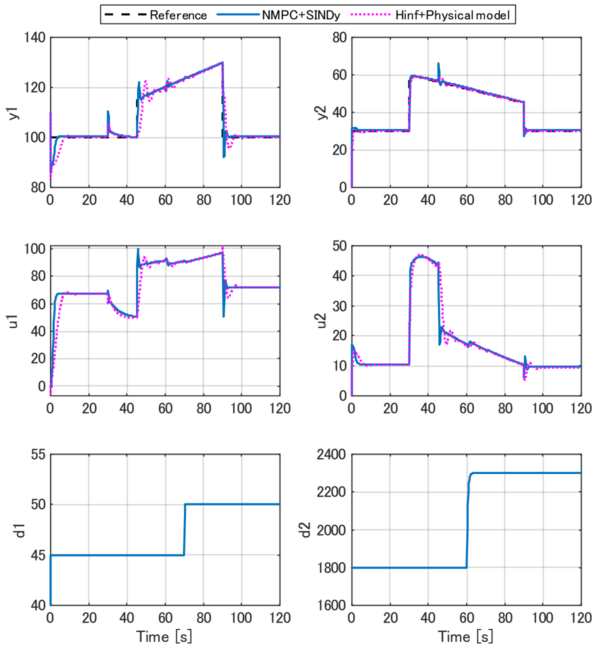

Fig. 5. Time-series data of NMPC and H_∞ control. y_1: boost pressure [kPa], y_2: EGR rate [%], u_1: VGT vane [%, closing], u_2: EGR valve [%, opening], d_1: fuel injection amount [mm^3/st], d_2: engine speed [rpm].

Table 6. MSEs under the NMPC and LTI controllers.

Controller	MSEs	
	Boost pressure	EGR rate
Offset-free NMPC	3.35	1.05
LTI H_∞ controller	11.5	1.24

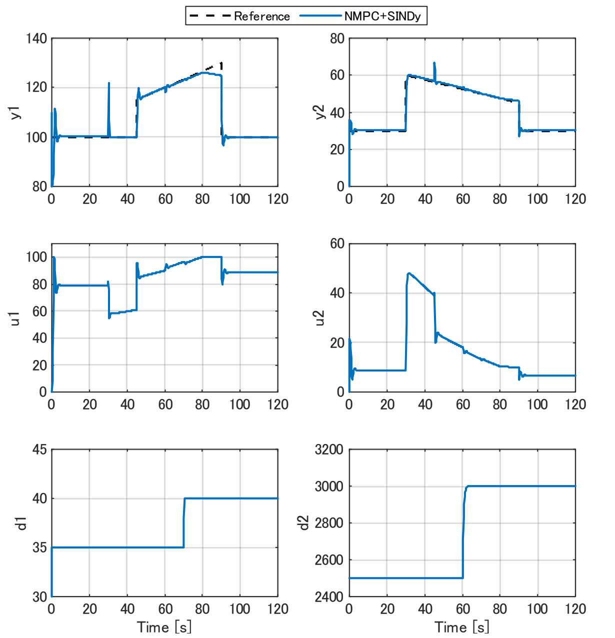

Fig. 6. Time-series data of NMPC to confirm actuator constraint. y_1: boost pressure [kPa], y_2: EGR rate [%], u_1: VGT vane [%, closing], u_2: EGR valve [%, opening], d_1: fuel injection amount [mm^3/st], d_2: engine speed [rpm].

5.3. Discussion

We investigated the effectiveness of the offset-free NMPC with the predictive model identified via SINDy for the diesel engine air path system, known as the nonlinear and complicated system. First, we applied the SINDy to the air path system, and accurate modeling was realized. The long-term prediction was examined in addition to the one-step prediction. Since the optimization problem (16) is based on the one-step-ahead evaluation, the long-term predictions may become low-accurate if the learning data is not rich enough. This paper considers the air path system of the MIMO complex nonlinear system; thus, the collected data may not be rich enough to create a data-driven model. Therefore, it is important to confirm the long-term prediction. In the simulation, R^2 values of the outputs (boost pressure and EGR rate) under long-term predictions were over 90% when λ is appropriately selected (see Table 3). Note that over 90% of R^2 is an acceptable value for many applications [44]. Additionally, we obtained the coefficient of the basis function (i.e., library) with a large influence on predictions from sparse identification results (see Fig. 4). Next, we constructed the NMPC with the prediction model obtained by SINDy. The augmented system (18) was also introduced to realize offset-free NMPC to remove steady-state error. The proposed NMPC (19) – (21) realized non-steady state error and actuator constraints under different operation conditions (see Fig. 5 and Fig. 6). Additionally, the NMPC provided better performance than the model-based LTI H_∞ controller which was designed using the nominal model with uncertainties (see Fig. 5 and Table 6). Specifically, the MSEs of the boost pressure under the proposed and conventional controllers are 3.35 and 11.5, respectively. The MSEs of the EGR rate under the proposed and conventional controllers are 1.05 and 1.24, respectively. Therefore, it can be confirmed that the proposed controller outperforms the conventional one. Note that the traditional model-based controller used in this simulation was designed by assuming that the physical mode is fully known. In the practical situation, the model-based design requires an accurate physical model; however, it is not easy to obtain an accurate physical model for nonlinear MIMO systems such as the air path system. On the other hand, NMPC with SINDy can be designed from only data under the condition that the plant model is unknown. From this perspective, the proposed data-driven method is superior not only in terms of control performance but also in terms of design cost compared to conventional model-based control design.

5. CONCLUSION

This paper has proposed an offset-free NMPC with the SINDy model, which is a novel data-driven approach, and applied it to the diesel engine air path system. In the system modeling, we introduce SINDy, which is one of the data-driven approaches, instead of physical modeling since SINDy provides high computational efficiency compared to neural networks and high modeling accuracy compared to physical modeling. The sparse model with low computational cost also leads to high compatibility with NMPC. In the NMPC design, we introduce offset-free NMPC to remove the steady-state error by adding the variable of integral error to the model obtained by SINDy. The simulation results revealed that SINDy provided a highly accurate sparse model, i.e., the R^2 values of the boost pressure and the EGR rate are over 90%, and NMPC performance outperformed the conventional model-base controller. To the best of the authors' knowledge, the study on NMPC with SINDy for diesel engines has not previously been conducted, and this study provides new insights for researchers and practical engineers. In the future, we will consider comparisons with other data-driven approaches such as Koopman modeling. Additionally, an experimental validation will be conducted.

APPENDIX A

We show the frequency characteristics instead of physical modeling. Fig. 7 depicts the frequency responses of the simulation model of the diesel engine air path system under various operating points (81 points in total) as shown in Table 7. From the figure, we can see that the diesel engine air path system is a complex MIMO system with strong nonlinearity. It is noted that the frequency characteristics are obtained by linearizing the original nonlinear system used in the simulation; thus, the original simulation model is more complicated than the linearized frequency characteristics.

Table 7. Operating points.

Parameter	Values		
VGT vane [%]	0	50	100
EGR valve [%]	0	50	100
Engine speed [rpm]	1000	2000	3000
Fuel injection amount [mm^3/st]	10	50	90

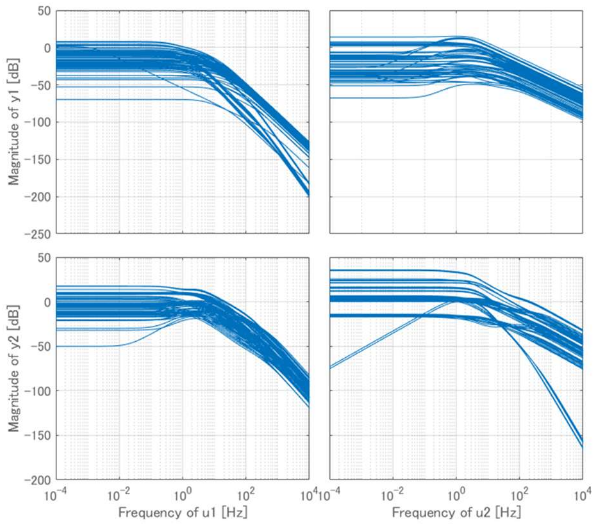

Fig. 7. Frequency characteristics of diesel engine air path system under various operating points.

CONFLICT OF INTEREST

The authors declare that they have no conflict of interest.

REFERENCES

[1] P. Van Overschee and B. De Moor, "N4SID: Subspace algorithms for the identification of combined deterministic-stochastic systems," *Automatica*, vol. 30, no. 1, pp. 75–93, Jan. 1994.

[2] K. Prag, M. Woolway, and T. Celik, "Toward Data-Driven Optimal Control: A Systematic Review of the Landscape," *IEEE Access*, vol. 10, pp. 32190–32212, 2022.

[3] M. C. Campi, A. Lecchini, and S. M. Savaresi, "Virtual reference feedback tuning: a direct method for the design of feedback controllers," *Automatica*, vol. 38, no. 8, pp. 1337–1346, Aug. 2002.

[4] S. Soma, O. Kaneko, and T. Fujii, "A new method of controller parameter tuning based on input-output data – Fictitious Reference Iterative Tuning (FRIT) –," *IFAC Proc. Vol.*, vol. 37, no. 12, pp. 789–794, Aug. 2004.

[5] A. Karimi, K. Van Heusden, and D. Bonvin, "Non-iterative data-driven controller tuning using the correlation approach," in *2007 European Control Conference (ECC)*, Kos, Greece, Jul. 2007, pp. 5189–5195.

[6] S. Yahagi and I. Kajiwara, "Direct Data-Driven Tuning of Look-Up Tables for Feedback Control Systems," *IEEE Control Syst. Lett.*, vol. 6, pp. 2966–2971, 2022.

[7] S. Yahagi and I. Kajiwara, "Direct tuning of gain-scheduled controller for electro-pneumatic clutch position control," *Adv. Mech. Eng.*, vol. 13, no. 8, pp. 1–12, Aug. 2021.

[8] S. Yahagi and I. Kajiwara, "Direct tuning method of gain-scheduled controllers with the sparse polynomials function," *Asian J. Control*, vol. 24, no. 5, pp. 2111–2126, Sep. 2022.

[9] S. Yahagi and M. Suzuki, "Controller parameter tuning for gain-scheduled vehicle yaw-rate control: Virtual reference feedback tuning approach," *Electron. Lett.*, vol. 59, no. 6, e12764, pp. 1–4, Mar. 2023.

[10] S. Yahagi and I. Kajiwara, "Data-driven design of model-free control for reference model tracking based on an ultra-local model: Application to vehicle yaw rate control," *Proc. Inst. Mech. Eng. Part J. Automob. Eng.*, Jan. 2024.

[11] S. Formentin, D. Piga, R. Tóth, and S. M. Savaresi, "Direct learning of LPV controllers from data," *Automatica*, vol. 65, pp. 98–110, Mar. 2016.

[12] T. E. Passenbrunner, S. Formentin, S. M. Savaresi, and L. Del Re, "Direct multivariable controller tuning for internal combustion engine test benches," *Control Eng. Pract.*, vol. 29, pp. 115–122, Aug. 2014.

[13] J. S. Kim, Y. S. Quan, and C. C. Chung, "Koopman Operator-based Model Identification and Control for Automated Driving Vehicle," *Int. J. Control Autom. Syst.*, vol. 21, no. 8, pp. 2431–2443, Aug. 2023.

[14] P. J. Schmid, "Dynamic mode decomposition of numerical and experimental data," *J. Fluid Mech.*, vol. 656, pp. 5–28, Aug. 2010.

[15] J. Peter Schmid and S. Joern, "Dynamic Mode Decomposition of numerical and experimental data," presented at the 61st Annual Meeting of the APS Division of Fluid Dynamics, San Antonio, Texas, 2008, vol. Volume 53, Number 15.

[16] S. L. Brunton, M. Budišić, E. Kaiser, and J. N. Kutz, "Modern Koopman Theory for Dynamical Systems," *SIAM Rev.*, vol. 64, no. 2, pp. 229–340, May 2022.

[17] M. Korda and I. Mezić, "Linear predictors for nonlinear dynamical systems: Koopman operator meets model predictive control," *Automatica*, vol. 93, pp. 149–160, Jul. 2018.

[18] S. Li, Z. Xu, J. Liu, and C. Xu, "Learning-based Extended Dynamic Mode Decomposition for Addressing Path-following Problem of Underactuated Ships with Unknown Dynamics," *Int. J. Control Autom. Syst.*, vol. 20, no. 12, pp. 4076–4089, Dec. 2022.

[19] S. L. Brunton, J. L. Proctor, and J. N. Kutz, "Discovering governing equations from data by sparse identification of nonlinear dynamical systems," *Proc. Natl. Acad. Sci.*, vol. 113, no. 15, pp. 3932–3937, Apr. 2016.

[20] E. Kaiser, J. N. Kutz, and S. L. Brunton, "Sparse identification of nonlinear dynamics for model predictive control in the low-data limit," *Proc. R. Soc. Math. Phys. Eng. Sci.*, vol. 474, no. 2219, p. 20180335, Nov. 2018.

[21] U. Fasel, E. Kaiser, J. N. Kutz, B. W. Brunton, and S. L. Brunton, "SINDy with Control: A Tutorial," in *2021 60th IEEE Conference on Decision and Control (CDC)*, Feb. 2021, pp. 16–21.

[22] S. Gupta and C. Rajhans, "Application of Quasi Infinite Horizon Nonlinear Model Predictive Control to Unstable Tank Reactor," *Int. J. Control Autom. Syst.*, vol. 21, no. 6, pp. 1840–1851, Jun. 2023.

[23] G. Zhu, H. Jie, and W. Hong, "Nonlinear Model Predictive Path Tracking Control for Autonomous Vehicles Based on Orthogonal Collocation Method," *Int. J. Control Autom. Syst.*, vol. 21, no. 1, pp. 257–270, Jan. 2023.

[24] J.-G. Sun, X.-F. Chen, G.-H. Su, M. Wang, and H.-G. Pan, "Multi-stage Nonlinear Model Predictive Control with Online Scenario Update for Semi-batch Polymerization Processes," *Int. J. Control Autom. Syst.*, vol. 20, no. 10, pp. 3187–3197, Oct. 2022.

[25] F. Deng, H.-L. Yang, L.-J. Wang, and W.-M. Yang, "UKF Based Nonlinear Offset-free Model Predictive Control for Ship Dynamic Positioning Under Stochastic Disturbances," *Int. J. Control Autom. Syst.*, vol. 17, no. 12, pp. 3079–3090, Dec. 2019.

[26] L. Ge *et al.*, "Simultaneous Stability and Path Following Control for 4WIS4WID Autonomous Vehicles Based on Computationally Efficient Offset Free MPC," *Int. J. Control Autom. Syst.*, vol. 21, no. 9, pp. 2782–2796, Sep. 2023.

[27] B. Bhadriraju, A. Narasingam, and J. S.-I. Kwon, "Machine learning-based adaptive model identification of systems: Application to a chemical process," *Chem. Eng. Res. Des.*, vol. 152, pp. 372–383, Dec. 2019.

[28] R. Subramanian, R. R. Moar, and S. Singh, "White-box Machine learning approaches to identify governing equations for overall dynamics of manufacturing systems: A case study on distillation

column," *Mach. Learn. Appl.*, vol. 3, p. 100014, Mar. 2021.
[29] A. Narasingam and J. Sang-Il Kwon, "Data-driven identification of interpretable reduced-order models using sparse regression," *Comput. Chem. Eng.*, vol. 119, pp. 101–111, Nov. 2018.
[30] F. Abdullah, Z. Wu, and P. D. Christofides, "Sparse-identification-based model predictive control of nonlinear two-time-scale processes," *Comput. Chem. Eng.*, vol. 153, p. 107411, Oct. 2021.
[31] K. Champion, P. Zheng, A. Y. Aravkin, S. L. Brunton, and J. N. Kutz, "A Unified Sparse Optimization Framework to Learn Parsimonious Physics-Informed Models From Data," *IEEE Access*, vol. 8, pp. 169259–169271, 2020.
[32] N. M. Mangan, S. L. Brunton, J. L. Proctor, and J. N. Kutz, "Inferring Biological Networks by Sparse Identification of Nonlinear Dynamics," *IEEE Trans. Mol. Biol. Multi-Scale Commun.*, vol. 2, no. 1, pp. 52–63, Jun. 2016.
[33] U. Fasel, J. N. Kutz, B. W. Brunton, and S. L. Brunton, "Ensemble-SINDy: Robust sparse model discovery in the low-data, high-noise limit, with active learning and control," *Proc. R. Soc. Math. Phys. Eng. Sci.*, vol. 478, no. 2260, p. 20210904, Apr. 2022.
[34] S. L. Brunton, J. L. Proctor, and J. N. Kutz, "Sparse Identification of Nonlinear Dynamics with Control (SINDYc)," *IFAC-Pap.*, vol. 49, no. 18, pp. 710–715, Jan. 2016.
[35] R. Moriyasu, S. Nojiri, A. Matsunaga, T. Nakamura, and T. Jimbo, "Diesel engine air path control based on neural approximation of nonlinear MPC," *Control Eng. Pract.*, vol. 91, p. 104114, Oct. 2019.
[36] S. Ishizuka, I. Kajiwara, J. Sato, Y. Hanamura, and S. Hanawa, "Model-free adaptive control scheme for EGR/VNT control of a diesel engine using the simultaneous perturbation stochastic approximation," *Trans. Inst. Meas. Control*, vol. 39, no. 1, pp. 114–128, Jan. 2017.
[37] M. Hirata, "H∞ Control of Diesel Engine Air Path System," *J. Soc. Instrum. Control Eng.*, vol. 59, no. 3, pp. 203–211, 2020.
[38] H. Xie *et al.*, "On Decoupling Control of the VGT-EGR System in Diesel Engines: A New Framework," *IEEE Trans. Control Syst. Technol.*, vol. 24, no. 5, pp. 1788–1796, Sep. 2016.
[39] S. Larguech, S. Aloui, O. Pagès, A. El Hajjaji, and A. Chaari, "Robust Adaptive Controller for the Diesel Engine Air Path with Input Saturation," *Int. J. Control Autom. Syst.*, vol. 17, no. 10, pp. 2541–2549, Oct. 2019.
[40] V. Aran and M. Unel, "Diesel Engine Airpath Controller Via Data Driven Disturbance Observer," *Int. J. Automot. Technol.*, vol. 21, no. 4, pp. 971–980, Aug. 2020.
[41] S. Kaneko *et al.*, *Model Based Control for Automotive engines*. CORONA, 2019.
[42] R. Tibshirani, "Regression Shrinkage and Selection Via the Lasso," *J. R. Stat. Soc. Ser. B Methodol.*, vol. 58, no. 1, pp. 267–288, Jan. 1996.
[43] D. Chicco, M. J. Warrens, and G. Jurman, "The coefficient of determination R-squared is more informative than SMAPE, MAE, MAPE, MSE and RMSE in regression analysis evaluation," *PeerJ Comput. Sci.*, vol. 7, p. e623, Jul. 2021.
[44] B. Schaible, Hong Xie, and Yung-Cheng Lee, "Fuzzy logic models for ranking process effects," *IEEE Trans. Fuzzy Syst.*, vol. 5, no. 4, pp. 545–556, Nov. 1997.

Shuichi Yahagi received the B.S. degree in Engineering from Shibaura Institute of Technology, Japan, and M.S. degree in Engineering from Hokkaido University, Japan, in 2011 and 2013, respectively. He joined ISUZU Advanced Engineering Center, Ltd. in 2013, and received Ph.D. degree in Engineering from Hokkaido University, Japan, in 2021. He is currently a Senior Research Engineer at the 6th Research Department, ISUZU Advanced Engineering Center, Ltd. His research interests include automobile control, data-driven control, model-free control, and PID control. He received the Asahara Science Award from the Society of Automotive Engineers of Japan and the Young Engineers Award from the Japan Society of Mechanical Engineers, in 2023 and 2024, respectively. His research has led to over 40 patents.

Hiroki Seto received the B.E. and the M.E. degrees in mechanical engineering from Nagaoka University of Technology, Japan, in 2004 and 2006, respectively. He received the Ph.D. in electric information and control engineering from Kanazawa University, in 2007. From 2007 until 2008, he was with Kyushu University as an Academic Fellow. In April 2008, he joined ISUZU Advanced Engineering Center, Ltd. His main research is the control algorithm of diesel engines and hybrid electric vehicles.

Ansei Yonezawa received the B.S., M.S., and Ph.D. degrees in engineering from Hokkaido University, Japan, in 2019, 2021, and 2023, respectively. From 2023 to 2024, he was a specially appointed Assistant Professor with the Graduate School of Engineering, Hokkaido University. Since 2024, he has been an Assistant Professor with the Faculty of Engineering, Kyushu University. His research interests include active vibration control, robust control, stochastic optimization, fractional-order control, and data-driven control. He received the Hatakeyama Prize and the Miura Prize given for best students in the field of mechanical engineering from the Japan Society of Mechanical Engineers, in 2019 and 2021, respectively.

Itsuro Kajiwara received the B.S. degree in engineering from Tokyo Metropolitan University, in 1986, and the M.S. and Ph.D. degrees in engineering from the Tokyo Institute of Technology, in 1988 and 1993, respectively. From 1990 to 2000, he was an Assistant Professor with the School of Engineering, Tokyo Institute of Technology, where he was an Associate Professor with the Graduate School of Engineering, from 2000 to 2008. Since 2009, he has been a Professor with the Graduate School of Engineering, Hokkaido University. His research interests include vibration, control, structural health monitoring, and laser application.